Stud. Univ. Babeş-Bolyai Math. 59(2014), No. 4, 543–556

Comparison of Riemann solvers in fluid dynamics by weighted error number

Csaba Müller and Lajos Gergó

Abstract. After using a numerical method our eyes are good witnesses whether that method is good or not. We aim to provide, for first order hyperbolic systems, a number that measures, determines the quality of a method instead of deciding by figures. This number is based on the ℓ_1 vector norm of the error vector, combined with weighting. This weight vector has bigger values near discontinuities and kinks because most of the Riemann-solvers have difficulties (including numerical diffusion and oscillations) in solving the equations near these states.

Mathematics Subject Classification (2010): 65M06.

Keywords: Riemann-solver, hyperbolic equation.

1. Introduction

Our primary research field is numerical methods for first order hyperbolic equations. This type of equations, systems are used in several places, for example in fluid dynamics, shallow water calculations, and many other places. For example if we want to model blood flow in human vascular system then the obtained equation will be hyperbolic too but a much more complicated one. For a detailed biomechanical view for this subject see [10].

In this case wall of veins can't be considered as a rigid tube, it is flexible, it can narrow and broaden. Thereby a new source term appears in the system which will depend on the solution itself. There is another big difficulty because in this case junctions have to be studied. In this paper we work with a simpler system of equations, namely the Euler system in fluid dynamics. For more detailed theory of hyperbolic equations see the Godlewski-Raviart book [3].

Our objective is to assign a number to a given numerical solution. This number should show us how that method can perform near critical regions. How close the numerical solution to the exact solution is; if the given method produces a solution at

This paper was presented at the 10th Joint Conference on Mathematics and Computer Science (MaCS 2014), May 21-25, 2014, Cluj-Napoca, Romania.

all. As we will see there are test cases where certain methods are unable to produce numerical results because of their properties. This is because most of the arising physical properties in modeling gas flows (pressure, density and energy) can't be negative. However in certain cases oscillations could occur with a portion of numerical methods. If these oscillations are big "enough" then they can reach negative region and a negative value in density for example ruins all the calculations.

These problems could be avoided by minor modifications of the methods but our goal is to use and study them in their "original" forms. We would do a note here. These methods usually lose slightly from their good properties due to the modifications and the running time could also increase by these extra checks.

1.1. Computer configuration used for tests

Hardware configuration.

- CPU: AMD FX-8350, 4.0-4.2 GHz
- RAM: 12 GB, DDR3-1600 MHz

Software configuration.

- Operating system: Microsoft Windows 7 (64-bit, Professional version)
- MATLAB version 2010b

2. Euler system

Our test equation is the Euler system in fluid dynamics. It is given as

$$\frac{\partial \vec{u}}{\partial t} + \frac{\partial \vec{f}(\vec{u})}{\partial x} = 0,$$

that is in the so-called conservative form. The solution vector $\vec{u}$ has three components, namely $\vec{u} = [\rho, m, e]$ where ρ is the density, $m = \rho u$ is the mass flow component and e is the total energy.

The function $\vec{f}$ is known as flux. It contains three components as

$$\vec{f}(\vec{u}) = \left[m, \quad \frac{m^2}{\rho} + p, \quad \frac{m}{\rho}(e + p) \right],$$

where p is the pressure. It can be calculated by the equation

$$e = \frac{p}{\gamma - 1} + \frac{m^2}{2\rho},$$

where γ is ratio of specific heats, a constant depending on the gas. In our tests we used $\gamma = 1.4$ which is the case of air.

Physically this system describes gas flow and state changes over time in a rigid one-dimensional tube with given initial values. It is easy to see that Euler system is nonlinear. Nonlinearity always brings additional complexity compared to the simpler linear cases. This is even more true in solving nonlinear partial differential equations numerically. In our case, complexity of the problem is caused by the nonlinearity of the flux and the discontinuity of initial values.

Characteristics are important in the case of hyperbolic equations (see [1], [12], [18]). In linear systems these characteristics are parallel lines. The components of the solution are constant along these lines, only depending on initial values and the source terms if the system is not homogeneous. Some methods were discussed by Roe [13] and LeVeque, Yee [9] for systems with source terms.

The aforementioned property also provides a simple method for calculating the solution, this is called the method of characteristics (see in [14]). The initial values should be moved along characteristic lines. Additionally if the system is inhomogeneous the source term should be integrated above a specific section of the characteristic line. In numerical mathematics there are many known methods to integrate a function above a finite line segment.

Characteristics are not parallel in the case of nonlinear equations. In addition they could intersect each other so we can not use this simple method.

But characteristics are still important in solving this system numerically. They describe the propagation speed of waves, S. If we want to guarantee stability for a numerical method then we should use a time step τ such that the following inequality holds in all grid points and for all coordinates

$$CFL := \frac{\tau\,|S|}{h} \leq c,$$

where h is the spatial step. The value of c is 1 for Lax-Friedrichs and Lax-Wendroff methods; it is $\frac{1}{2}$ for Godunov-type methods, so that the waves do not cross the cell borders (see [18]). CFL (Courant-Friedrichs-Levy) is called Courant number.

So the stability of a method depends on the Courant number, therefore we need to determine this number during calculations. Because τ and h depends only on discretization, we need to calculate S in all grid points.

This value S depends on none other than the eigenvalues of Jacobian matrix of the flux which is nothing other than the slope of characteristics. In linear case, these eigenvalues are constant, but in our case they depend on the solution as well.

Analytically the eigenvalues of the Euler system are as follows

$$\lambda_1 = u - c, \lambda_2 = u, \lambda_3 = u + c,$$

where u is the velocity of the gas and c is the speed of sound which can be calculated by

$$c = \sqrt{\gamma \frac{p}{\rho}}\,.$$

We determine approximation to this number in all grid points during the entire calculation and examine whether the maximal absolute value from these numbers meets the Courant condition or not. In practice this is the easiest way to guarantee the stability.

3. Test cases

In our tests we solved the Euler equation with different initial values (see Table 1). These initial values are from the book of Toro [18]. We assume that the initial values consist of two different constant states with a discontinuity in x_0 as follows

$$\vec{u}_0(x) := \vec{u}(x,t)\,|_{t=0} = \begin{cases} [\rho_L, m_L, e_L]^T \,(=: \vec{u}_L) & \text{if } x < x_0 \\ [\rho_R, m_R, e_R]^T \,(=: \vec{u}_R) & \text{if } x_0 < x \end{cases}$$

where the indices L and R refer to the left and right constant states.

For this special type of initial conditions the initial value problem is called Riemann problem. The spatial domain is taken as interval $[-3, 3]$ and our time domain is $[0, T]$ where T is a parameter of the test case. The calculations were done on a finite interval so we need boundary conditions. In our cases we used transmissive boundary conditions (see [2]). The spatial domain was divided to 600 subintervals, so h is fixed at 0.01 in all cases. Time steps number M could be changed in order to guarantee stability. Then

$$\tau = \frac{T}{M}$$

can be applied to determine time step size.

The spatial-time graph can be divided into 4 parts in the case of Riemann problem by 3 lines. In all subparts of the graph, gas states (velocity, pressure, density and energy) are constant.

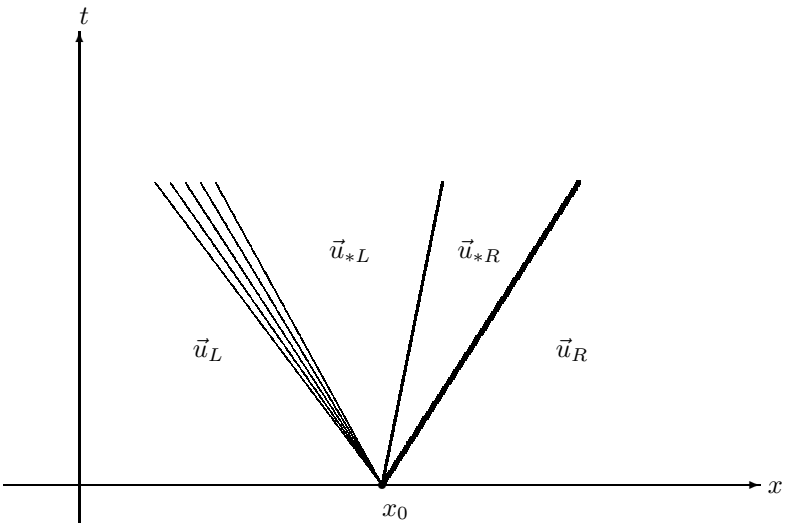

FIGURE 1. Characteristic types

These three lines are characteristic lines starting from the discontinuity of initial values (see Figure 1). There are three different types of characteristics. There is a conventional way of marking these waves by type. Thick lines mark the so-called shock waves, thinner lines mark the contact discontinuity in the middle and the fan-like marking is for rarefaction waves. For more detailed descriptions of waves, see the book of Whitham [20].

In our case the middle wave will be a contact wave. Only density and total energy change along a contact wave, velocity and pressure are equal on both sides of this wave. The region between the two outer waves is called star region.

It is important to note that while contact and shock waves produce a discontinuity in solution, rarefaction waves do not. They blur and link the values from the adjacent regions continuously. This is the reason of the fan-like marking in figures.

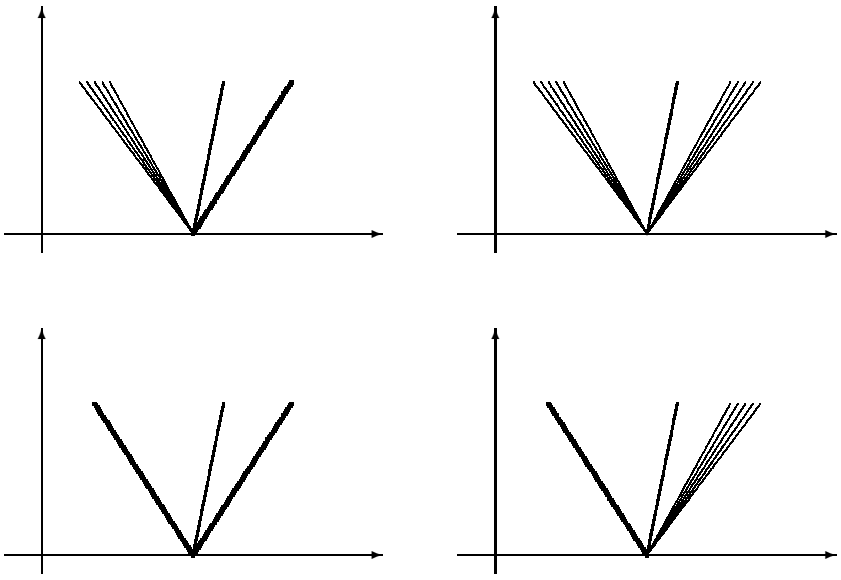

FIGURE 2. Possible characteristic layouts

On our example graph there is a rarefaction wave on the left side and a shock wave on the right. There are 4 possible layout as you can see in figure 2. On a given side the wave type depends on how the pressure on that particular side compares to the pressure in star region. If pressure is higher in the star region then there will be a shock wave at a given side , if lower (or equal) then there will be a rarefaction wave.

After presenting the wave types and possible layouts we describe each test cases in a few words.

Test	x_0	T	ρ_L	u_L	p_L	ρ_R	u_R	p_R
1	0	1	1	0	1	0.125	0	0.1
2	−1.2	1.2	1	0.75	1	0.125	0	0.1
3	0	0.9	1	−2	0.4	1	2	0.4
4	0	0.072	1	0	1000	1	0	0.01
5	−0.6	0.21	5.99924	19.5975	460.894	5.99242	−6.19633	46.095
6	1.8	0.072	1	−19.59745	1000	1	−19.59745	0.01
7	0	12	1.4	0	1	1	0	1
8	0	12	1.4	0.1	1	1	0.1	1

TABLE 1. Initial values and parameters

Test case 1 is a very popular test case for this equation, called SOD test case. Its characteristics layout is the same as in figure 1, so there is a rarefaction wave on the left, middle wave is contact discontinuity. This is moving to the right slowly by the time. The right wave is a shock wave in this case.

Test case 2 is very similar to test 1, but the initial velocity isn't 0 on the entire interval, only on the right side, it is 0.75 on the left. Wave structure is the same as in test 1 but wave slopes, speeds differ from those. Numerical results are also very similar.

In test case 3 there are two rarefaction waves symmetrically to 0. These rarefactions cover two long intervals. Generally, numerical methods do not handle these long rarefaction waves well. Furthermore close to vacuum state appears in this test, which causes the Lax-Wendroff method to fail.

The wave layout in test 4 is the same as in test 1 and 2 but in this case contact and shock waves are extremely close to each other. Robustness of the method can be measured by this test case. Initial values differ several orders of magnitude on two sides which causes another difficulty to numerical methods.

Test 5 is very similar to test 4 but in this case left wave will also be a shock wave and there will be bigger distance between contact discontinuity and right shock wave. Numerical results are also similar to those seen in the latest test.

Test 6 is almost exactly the same as test 4 except the initial velocity is not 0. Perhaps the biggest differences are visible among methods in this test case. Because of this we make a comparative figure (see Figure 3) for the obtained numerical approximations by different methods. We only represent the density plots since density graph is always the most interesting one.

Test 7 is a trivial test case, because the gas is in steady state. There is one trivial rarefaction wave on both sides. The contact wave stays at $x_0 = 0$ and does not move, however bunch of numerical methods blur this discontinuity along left and right states because of numerical diffusion. Some methods can produce exact solution in this case because of the simplicity of initial values and trivial wave structure.

Test 8 is almost the same as case 7, except the contact wave will move to the right slowly by the time. The results are also very similar to those produced in the latest test case, but there is no method producing exact solution.

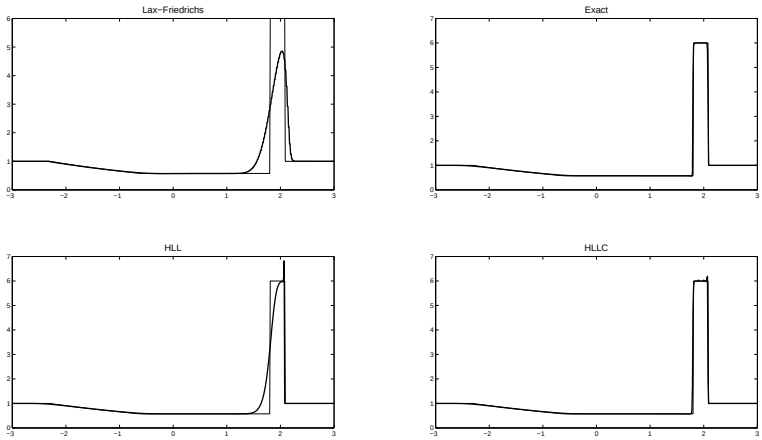

FIGURE 3. Test 6: obtained density plots by different methods

4. Approximate Riemann-solvers

We study conservative numerical methods in the following form

$$\vec{u}_i^{j+1} = \vec{u}_i^j - \frac{\tau}{h}\left(\vec{f}_{i+\frac{1}{2}}^{j+\frac{1}{2}} - \vec{f}_{i-\frac{1}{2}}^{j+\frac{1}{2}}\right),$$

where $\vec{u}_i^j$ means the numerical approximation at time level j in the ith spatial point and $\vec{f}_{i\pm\frac{1}{2}}^{j+\frac{1}{2}}$ is the left and right intercell numerical flux. The studied methods differ only in the calculation, definition of this numerical flux.

The basic idea comes from Godunov [4]. The initial value problem could be solved by calculating exact or approximate solution of a Riemann problem in each cell of the grid. We get the intercell numerical fluxes from these solutions. Then we can do a time-step.

Five different Riemann-solvers were tested, the Lax-Friedrichs, Lax-Wendroff, HLL solver, HLLC solver, and the exact one. Intercell flux can be expressed without solving a Riemann problem in the case of Lax-Friedrichs and Lax-Wendroff solvers.

The Lax-Friedrichs [7] solver has an important advantage over the other (except the exact) solvers, namely this is a monotone solver. Therefore it will not produce oscillations near the regions with difficulties, according to Godunov's theorem (see [4]). On the other hand it has a disadvantage, it generates a high numerical diffusion near the contact discontinuity.

The Lax-Wendroff [8] solver is second order for linear problems, and therefore it can not be monotone method, so it will produce oscillations near the discontinuities. It is a disadvantage, but on the other hand it limits the discontinuities to a smaller interval. It means that the numerical diffusion will be much smaller using Lax-Wendroff scheme than in the case of using a first order methods.

The other three tested methods are really based on Riemann problem. The HLL solver [6] uses approximations to the two outer waves' speed only. It has problems with middle wave, in the form of high numerical diffusion. The HLLC solver is an improved version of the HLL solver introduced by Toro [17]. It tries to reduce numerical diffusion in the way of using estimates for all three wave speeds, C refers to the contact.

Finally the exact Riemann solver. It computes the exact solution of the Riemann subproblems. There are many works related to the exact solver, for example [4], [5], [11], [15], [16] and [19]. We used the version from [18, Chap. 4].

5. Numerical results

All test cases (see Table 1) were computed by all the mentioned numerical methods and all of the obtained approximations were studied.

All of our test cases are Riemann problems. There exists exact solver for these type of problems, as mentioned above. This can be used to compare the obtained numerical approximations to the exact solution.

Our primary goal is to specify the error at time T as follows

$$\|\vec{u}(\cdot,T) - \vec{u}_{num}(\cdot,T)\|_{L_1} = \int_{-3}^{3} |\vec{u}\,(x,T) - \vec{u}_{num}\,(x,T)|\ \mathrm{d}x, \tag{5.1}$$

this is the L_1 norm of the difference between the exact and the approximate solution, where $\vec{u}_{num}$ is the numerical solution. But numerical solution gives values only in grid points, therefore we can not integrate this difference along the specified interval. We could interpolate the numerical values and then integrate using this interpolation, but there is a more simple way.

We evaluate the exact solution only in grid points at time level T, denote this vector of values by $\vec{U}^{(i)}_{exact}$, $(i = 0, 1, \ldots 600)$. Then we can get the discretization of L_1 norm by calculating the

$$\left\|\vec{U}_{exact} - \vec{U}_{num}\right\|_{\ell_1} = \sum_{i=0}^{600} \left|\vec{U}^{(i)}_{exact} - \vec{U}^{(i)}_{num}\right|$$

ℓ_1 vector norm, where $\vec{U}^{(i)}_{num}$ is the numerical solution at time level T in the ith spatial grid point. The $\vec{U}^{(i)}_{exact}$ and $\vec{U}^{(i)}_{num}$ contains multiple values, so these calculations could be made coordinate-by-coordinate.

We remark here that if we use interpolation to calculate the error formula (5.1) then the results would be almost the same. For example if we use the trapezoidal rule then the result differs only by a multiplication factor of h, because at the boundaries the error is 0, at the inner points the trapezoidal rule multiplies by h.

It is not our goal. We want to calculate the error with higher weights near critical regions. For this reason our exact solver returns the types and places of waves at time $t = T$. The mentioned critical regions are the locations of contact, shock waves and head and tail of rarefaction waves at time $t = T$.

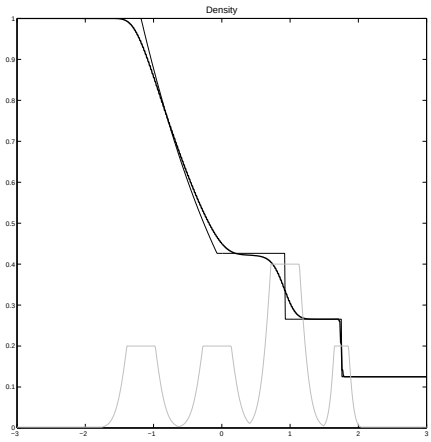

FIGURE 4. Weight vector on the density plot

Weights are developed as follows. We use

$$w(x) = min\left\{c_1 e^{-c_3\,(x-c_2)^2};\ c_4\right\}, \quad x \in [-3, 3]$$

functions. 3 to 5 functions of this type and the constant 1 function were taken. Then the weight in the ith point of the grid (w_i) is the maximal value of the previous functions' value in that given point.

It should be noted that we have actually two different weight vectors because contact discontinuity only appears in the density and total energy graphs. One of the weight vectors is used to these coordinates. The other weight vector ignores the contact wave. We use this to calculate error of the pressure and velocity components.

We tuned the constants $(c_1, \ldots, c_4)$ to focus weights to critical regions. Based on our experience we use 3 truncated exponential functions. The function

$$min\left\{200\, e^{-64\,(x-c)^2}, 100\right\}$$

is used in case of shock waves where c is the place of shock at time $t = T$;

$$min\left\{200\, e^{-16\,(x-c)^2}, 100\right\}$$

is used to the head and tail of a rarefaction wave, c is the place of the head/tail of the given rarefaction;

$$min\left\{400\, e^{-64\,(x-c)^2}, 200\right\}$$

is used to contact discontinuities, c denotes the place of the contact wave. In all function x takes value from the $[-3, 3]$ interval.

Test	Lax-Friedrichs	Lax-Wendroff	HLL	HLLC	Exact
1	0.0294	0.0075	0.0156	0.0151	0.0144
	0.0163 s	0.0401 s	2.8603 s	3.0637 s	91.5954 s
2	0.0413	0.0096	0.0160	0.0162	0.0163
	0.0373 s	0.0598 s	4.2828 s	4.5213 s	126.875 s
3	0.0193	–	0.0237	0.0237	0.0214
	0.0303 s	–	3.0494 s	3.1376 s	98.2901 s
4	47.2754	–	28.2834	27.9647	27.8372
	0.0409 s	–	5.0140 s	5.3397 s	129.833 s
5	86.1165	–	30.2774	31.0984	30.307
	0.0627 s	–	7.7901 s	8.0085 s	276.242 s
6	14.0664	–	11.1666	10.2964	9.5426
	14.0664 s	–	5.3077 s	5.5960 s	130.901 s
7	0.0323	$\approx 10^{-16}$	0.0316	0	0
	0.0934 s	0.1540 s	18.4428 s	19.5587 s	819.263 s
8	0.0329	0.0088	0.0318	0.0131	0.0131
	0.1132 s	0.1779 s	20.091 s	21.174 s	657.2296 s

TABLE 2. Summary of results

Figure 4 illustrates the resulting weight vector with the exact solution and a numerical approximation by Lax-Friedrichs solver of the density plot for SOD test case. In the figure thinner line marks the exact solution, the thicker one marks the numerical approximation while the lighter line marks the weight vector scaled down by 500.

Then the weighted error is defined in the following steps. First we calculate the

$$error_w = \frac{1}{W} \sum_{i=0}^{600} w_i \, |numerical_i - exact_i|$$

numbers for all coordinates where $W = \sum_{i=0}^{600} w_i$ with the corresponding weight vector's values. To be totally clear $numerical_i$ marks the given coordinate of the numerical approximation in ith grid point, $exact_i$ stays for the exact solution in that point. After calculating this number for all four coordinates we average these to get the final weighted error of the approximation.

We summarize these results in Table 2. There are two numbers in each cell of this table. Weighted error numbers are at top and the runtimes are at bottom of each cell.

Each test was calculated with the highest possible Courant number that holds stability. We get the slightest numerical diffusion this way.

We examined how methods work if using not 1 but 0.75, 0.5 and 0.25 as Courant numbers. You can find these results in Table 3 using Lax-Friedrichs method.

Results get worse in all test cases, because more time-steps should be done to reach the desired $t = T$ level as we have smaller time step size.

We make another figure (Figure 5) to illustrate this behavior. On all of these figures thinner line marks the exact solution, thicker one marks the numerical solution using the Lax-Friedrichs method with the corresponding CFL number can be found

Test	$CFL \leq 1$	$CFL \leq 0.75$	$CFL \leq 0.5$	$CFL \leq 0.25$
1	0.0294	0.0394	0.0546	0.0836
2	0.0413	0.0523	0.0702	0.1049
3	0.0193	0.0364	0.0566	0.0897
4	47.2754	58.7429	74.6345	99.69
5	86.1165	112.4286	157.1259	239.5929
6	14.0664	23.4655	34.5278	54.0884
7	0.0323	0.0342	0.0366	0.0399
8	0.0329	0.0348	0.0372	0.0404

TABLE 3. Lax-Friedrichs method with different Courant numbers

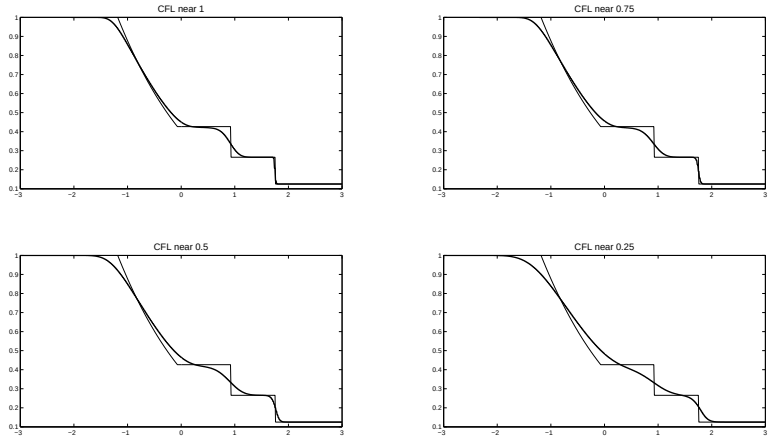

FIGURE 5. Test 1 with different Courant numbers using Lax-Friedrichs method

in the title of the subfigure. We mentioned that doing more time steps increases numerical diffusion. For example when CFL is near 0.25 then the obtained solution is almost a straight line between side states. It is impossible to recognize discontinuities based on this approximation.

These modified CFL tests were done with Lax-Wendroff method. In this case numerical diffusion grow only slightly but oscillations increasing and widening (see Figure 6). In this figure thinner line marks the exact solution, thicker line marks the numerical approximation using the Lax-Wendroff method with CFL number as in the title of the subfigure.

The other three methods do not produce worse solutions (maybe a little bit worse, barely visible differences) calculating with lower Courant number. The reason of this could be that they divide the whole problem to many Riemann problems and they use some approximation of wave speeds. They can keep numerical diffusion under control this way.

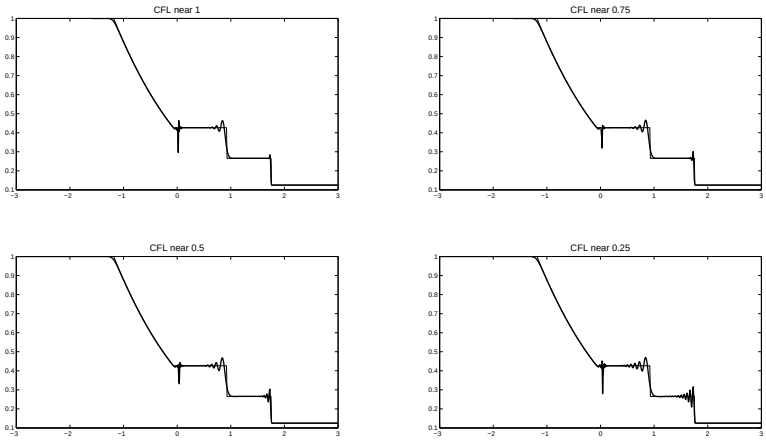

FIGURE 6. Test 1 with different Courant numbers using Lax-Wendroff method

6. Remarks and conclusion

The space step size, h was fixed at 0.01 in all of our tests. We remark that in the case we use a smaller space step our results will keep the same pattern. Of course the approximations would be more accurate, numerical diffusion and oscillations would take a narrower interval. But we should take more time steps in order to keep the CFL number below 1 and therefore computational time would increase significantly. For example if we use half of the original spatial step size ($h = 0.005$), it means twice as much intervals as in the original case, but we should take about twice as much time steps because of the CFL condition. So the calculation time increases with a multiplier of 4, but the accuracy of the approximation would not be 4 times better. All in all taking a fixed h was just a simplification to our test procedure.

The runtime of the exact solver is incredibly high in comparison with other solvers. That is because it has to calculate the exact solution of a Riemann problem in each cell. Which is a very time-consuming task. In addition we can see that its weighted error values are not much better compared for example to the $HLLC$ solver's values. So using the exact solver is only recommended for very sharpened cases.

Lax methods are much quicker than their counterparts in all cases. The explanation is simple, these two solvers could be written in a closed formula, as mentioned above, so they actually do not need to divide the problem into subproblems thus considerably simplifying the process of calculation.

Furthermore, we remark that in general cases we do not have an exact solver, so we can not produce exact solution. We could not compare our results to the exact

solution. In this case we should make a quasi-exact solution using some monotone (eg. Lax-Friedrichs) method with very fine spatial discretization. Numerical diffusion should be corrected after the calculation in order to use this as a quasi-exact solution and compare other methods to this result.

References

[1] Dafermos, C.M., *Generalized characteristics in hyperbolic systems of conservation laws*, Archive for Rational Mechanics and Analysis, **107**(1989), 127–155.

[2] Giles, M.B., *Non-reflective boundary conditions for euler equation calculations*, AIAA Journal, **28**(1990), 2050–2058.

[3] Godlewski, H., Raviart, P.A., *Numerical Approximation of Hyperbolic Systems of Conservation Laws*, Springer, 1996.

[4] Godunov, S K., *A finite difference method for the computation of discontinuous solutions of the equations of fluid dynamics*, Mat. Sb., **47**(1959), 357–393.

[5] Gottlieb, J.J., Groth, C.P.T., *Assessement of riemann solvers for unsteady one-dimensional inviscid flows of perfect gases*, J. Comput. Phys., **78**(1988), 437–458.

[6] Harten, A., Lax, P.D., van Leer, B., *On upstream differencing and godunov type methods for hyperbolic conservation laws*, SIAM Rev., **25**(1983), 35–61.

[7] Lax, P.D., *Weak solutions of nonlinear hyperbolic equations and their numerical computation*, Comm. Pure Appl. Math., **7**(1954), 159–193.

[8] Lax, P.D., Wendroff, B., *Systems of conservation laws*, Comm. Pure Appl. Math., **13**(1960), 217–237.

[9] LeVeque, R., Yee H.C., *A study of numerical methods for hyperbolic conservation laws with source terms*, J. Comp. Phys., **86**(1990), 187.

[10] Parker, K.H., Jones, C.J.H., *Forward and backward running waves in the arteries: Analysis using the method of characteristics*, Journal of Biomechanical Engineering, **112**(1990), 322–326.

[11] Pike, J., *Riemann solvers for perfect and near-perfect gases*, AIAA Journal, **31**(10)(1993), 1801–1808.

[12] Roe, P.L., *Characteristic-based schemes for the euler equations*, Ann. Rev. Fluid Mech., **18**(1986), 337–365.

[13] Roe, P.L., *Upwind differenced schemes for hyperbolic conservation laws with source terms*, In Proc. Conf. Hyperbolic Problems, (Carasso, Raviart, Serre editors), Springer, 1986, 41–51.

[14] Sarra, S.A., *The method of characteristics with applications to conservation laws*, JOMA, **3**(2003).

[15] Schleicher, M., *Ein einfaches und effizientes verfahren zur loesung des riemann-problems*, Z. Flugwiss. Weltraumforsch., **17**(1979), 265–269.

[16] Toro, E.F., *A fast riemann solver with constant covolume applied to the random choice method*, Int. J. Meth. Fluids, **9**(1989), 1145–1164.

[17] Toro, E.F., Spruce, M., Speare, W., *Restorian of the courant surface in the hll-riemann solver*, Shock Waves, **4**(1994), 25–34.

[18] Toro, E.F., *Riemann Solvers and Numerical Methods for Fluid Dynamics*, Springer, 3rd edition, 1999.

[19] van Leer, B., *Towards the ultimate conservative difference scheme v. a second order sequel to godunov's method*, J. Comput. Phys., **32**(1979), 101–136.

[20] Whitham, G.B., *Linear and Nonlinear Waves*, John Wiley & Sons, 1999.

Csaba Müller
Eötvös Loránd University
Faculty of Informatics
1/C, Pázmány Péter sétány
1117 Budapest, Hungary
e-mail: csaba108@gmail.com

Lajos Gergó
Eötvös Loránd University
Faculty of Informatics
1/C, Pázmány Péter sétány
1117 Budapest, Hungary
e-mail: gergo@cs.elte.hu